

## Fast and sensitive THz detector based on miniaturized optomechanical resonator

---

*Jiawen Liu<sup>1\*</sup>, Baptiste Chomet<sup>1</sup>, Djamel Gacemi<sup>1</sup>, Konstantinos Pantzas<sup>2</sup>, Grégoire Beaudoin<sup>2</sup>, Isabelle Sagnes<sup>2</sup>, Angela Vasanelli<sup>1</sup>, Carlo Sirtori<sup>1</sup> and Yanko Todorov<sup>1</sup>*

<sup>1</sup> *Laboratoire de Physique de l'Ecole Normale Supérieure, ENS, Université PSL, CNRS, Sorbonne Université, Université de Paris, Paris, France*

<sup>2</sup> *Centre de Nanosciences et de Nanotechnologies (C2N), CNRS—Université Paris-Sud/Paris-Saclay, Palaiseau 91120, France*

---

*Keywords: THz detection; optomechanical resonator; dielectric gradient force; thermal effect*

---

### Abstract/Résumé

The development of technologies at the terahertz frequency domain requires fast, sensitive THz detectors working at room temperature. Here we demonstrate a miniaturized resonator with a suspended beam that acts as a mechanical oscillator converting THz signals into mechanical oscillations at megahertz frequency. Thanks to the optimized thermomechanical effect on our resonators, they respond very strongly to the incident THz radiation with a responsivity of 4 nm/μW, and thus can be employed as sensitive THz detectors operating at room temperature. We further implement phase lock loop (PLL) measurements which show that the device can respond at high speed, on the order of 1 MHz, limited by the cut-off frequency of PLL. In addition to the terahertz detection, our system can also serve as a great platform for fundamental research when the mechanical oscillation is forced into a strong non-linear regime by an external drive. This effect can also be exploited to build reconfigurable logic gates for THz signal processing, which is studied in our ongoing work.

### 1 Introduction

The Terahertz (THz) frequency domain can be the playground for many applications, such as wireless THz communications [1], imaging and bio-chemical sensing [2][3]. Nowadays, sensitive commercial THz detectors mostly depend on thermal effects, whose speed is slow and many of them need to operate at low temperature [4]. Recently, advanced THz detectors based on thermal effects have been reported by different groups, using metamaterial absorbers [5], micro-electromechanical systems (MEMS) [6] etc. However, the potential of this scheme is still not achieved yet: one can improve the response speed by miniaturizing the dimensions of the devices [7,8], and enhance the responsivity by exploiting better the thermal effects.

In this paper, we combine THz resonators with micro-mechanical oscillators to create a miniaturized optomechanical device, which is designed in a dog-bone shape with a bi-material structure consisting of a gold layer on top of the GaAs. In this structure, the gold resonator will act as a receiving antenna to resonantly absorb THz light and then heat up the system. The suspended thin beam of dog-bone will work as a thermal-sensitive mechanical oscillator, whose vibration frequency, amplitude and phase respond strongly to the heat in the system generated by the THz radiation. We supplement our device with micro-electrodes to drive individual mechanical oscillators using dielectric gradient forces [9], which allows, for example, the establishment of a phase lock loop (PLL) to study the response rates of our device. Thanks to these optimizations, we systematically demonstrate here an ultrafast sensitive THz detector based on thermal effects working at room temperature.

### 2 Results

Our optomechanical device, as presented in Figure 1, consists of two anchoring pillars and a suspended doubly-clamped beam with length  $l = 17 \mu\text{m}$  and width  $w = 250 \text{ nm}$ . To optimize the thermomechanical effect, a bi-material structure is employed, composed of a layer of gold (thickness  $u_{Au} = 150 \text{ nm}$ ) deposited on top of GaAs ( $u_{GaAs} = 200 \text{ nm}$ ). The total thickness of the suspended beam is thus  $u = 350 \text{ nm}$ . These dimensions are carefully designed so that the device can efficiently interact with the incident THz radiation from a quantum

cascade laser (QCL), which induces a strong eddy current on the thin beam and generate thermal strains thanks to different thermal expansion coefficients of the gold and GaAs. Therefore, by probing the mechanical motion of a single device, one can get access to the information of the incident THz signal.

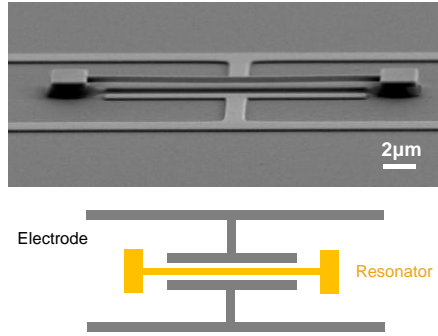


Figure 1: SEM image and top-view sketch of a dog-bone resonator with RF electrodes.

A homebuilt microscope is employed to measure the mechanical motion of the beam by an optical read-out method (the schematic of the setup can be found in Ref. [7]). We focus a near-infrared laser beam ( $\lambda=930$  nm) onto a single device and collect the backscattered laser light by a microscope objective. The mechanical oscillations of the beam are thus imprinted on the intensity modulation of the laser beam and can be measured on the RF spectrum of a spectrum analyser connected to the balanced photodiode unit. Figure 2a (blue curve) shows the experimental Brownian motion peak induced by the thermal noise from the surrounding environment, which can be well fitted in Figure 2c by the sum (red curve) of a Lorentzian distribution (orange dashed line) and a noise floor (black dashed line). This peak is measured at 2.87 MHz with a quality factor of  $\sim 1000$  at a low pressure of 1 mbar, corresponding to the fundamental out-of-plane flexural vibration mode of the beam, as visualized by the FEM simulation in Figure 2c. Importantly, Brownian motion peak can be exploited for calibration of the mechanical response [7,10]: by relating its power density spectrum to the thermal energy  $k_B T$  (where  $k_B$  is the Boltzmann constant and  $T$  is the temperature), one can convert the measured signal from voltage power spectral density ( $V^2/Hz$ ) to the motion power spectral density ( $pm^2/Hz$ ), from which the displacement of the mechanical beam is accessible.

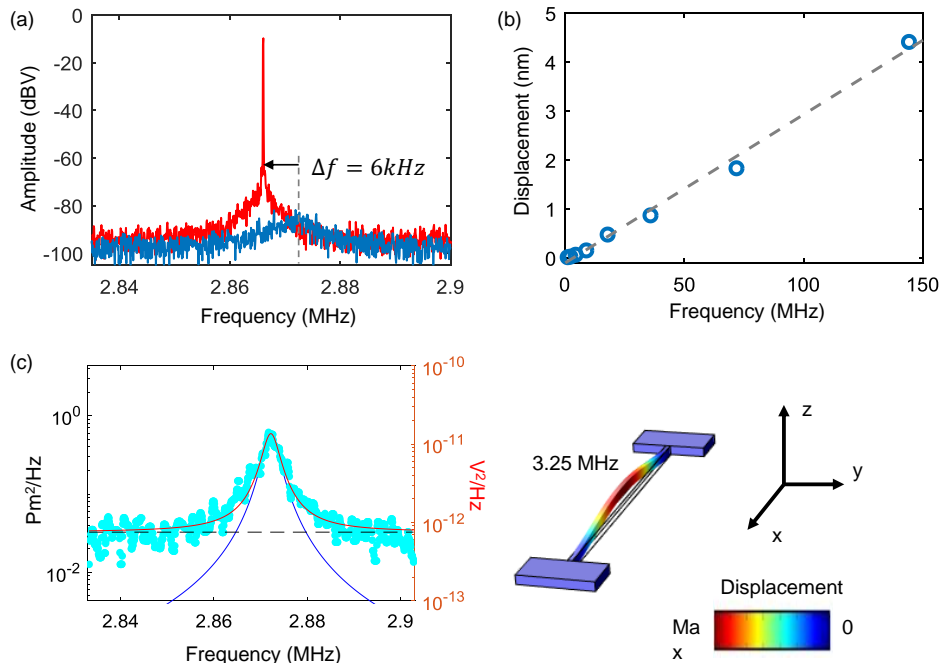


Figure 2: (a) Measured Rf spectra in the presence (red) or absence (blue) of the THz radiation (b) Linear correlation between the displacement of the vibrating beam and the QCL power. The external responsivity is  $15 pm/\mu W$ . (c) The experimental Brownian motion spectrum (Blue dots, measured with 100 Hz resolution bandwidth) can be well fitted by a sum of a Lorentzian distribution (blue solid line) and a noise floor (black dashed line). FEM simulation indicates that this mode corresponds to the fundamental out-of-plane flexural vibration mode.

Next, we shine the THz light onto the sample and measure the resulted spectrum. We use a RF generator to modulate the driving current of our QCL and obtain an output power expressed as  $P_{QCL} = \frac{P_0}{2} [1 + \cos(\omega_m t)]$  where  $P_0 \sim 1.2 \text{ mW}$  is the peak power and  $\omega_m$  is the modulation frequency that is close to the mechanical mode of the beam. In this case, a sharp peak signal is detected, with a contrast of about 60 dB to the Brownian thermal noise. Then we use paper filters to gradually attenuate the power  $P_0$  down to  $1 \mu\text{W}$  and summarize the amplitude responses as a function of the power of THz radiation in Figure 2b, from which an external responsivity of  $15 \text{ pm}/\mu\text{W}$  can be extracted. In addition to the amplitude response, Figure 2a also shows that the Brownian motion peak will shift to a lower frequency because of the thermal expansion in the presence of the THz radiation. Therefore, one can deduce the absorbed power  $P_{abs}$  in the mechanical beam from this frequency shift  $\Delta f$ . These two values are linked by a formula  $P_{abs} = \frac{6\alpha\lambda_T}{l} \Delta T$ , where  $\lambda_T \sim 163 \text{ W m}^{-1} \text{ K}^{-1}$  is the average thermal conductivity of the beam and  $\Delta T = \frac{1}{C_T} \frac{\Delta f}{f_0}$  is the temperature rise in which  $C_T \sim 0.005/\text{K}$  represents the temperature-frequency coefficient [11,12]. In the present case, the frequency shift  $\Delta f \sim 6 \text{ kHz}$  corresponds to a temperature change of  $0.42 \text{ K}$  and thus the absorbed power  $P_{abs}$  is estimated to be  $2.1 \mu\text{W}$ . This result yields a coupling efficiency for a single device  $P_{abs}/P_{QCL} \sim 0.35\%$  and an internal responsivity  $\sim 4 \text{ nm}/\mu\text{W}$ .

The response speed of the device can be measured with the help of a phase-lock loop (PLL) [6]. The feedback of the loop is enabled here by the dielectric driving scheme [9]. In this scheme, the oscillating beam is driven by a RF field through the micro-electrodes, with a voltage of  $1 \text{ V}$  and a frequency close to the mechanical mode  $f_m$ . The detected signal is sent back to the phase lock loop to stabilize its frequency. When THz radiation is shined onto resonators, the initial vibration frequency  $f_m$  will be shifted by  $\Delta f_m$ , which will be detected by the PLL and then be converted into an output signal.

During the measurements, we sweep the modulation frequency of the QCL over a wide range, from  $1 \text{ kHz}$  to  $8 \text{ MHz}$  and plot the response amplitude in figure 3a (orange curve). As a result, the response signal is about  $50 \text{ dB}$  as compared to the noise floor (below  $-100 \text{ dBV}$ ), remaining constant until the modulation frequency reaches the cut-off of the PLL ( $\sim 1 \text{ MHz}$ , gray curve). Therefore, the detection speed of the system can reach  $1 \text{ MHz}$ , limited by the PLL's transfer bandwidth.

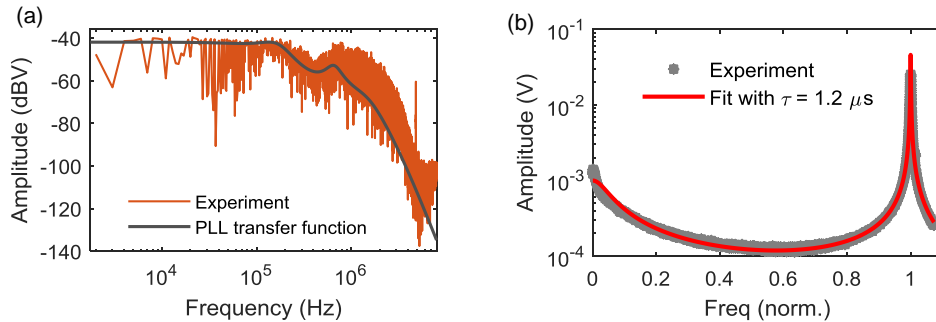


Figure 3: (a) Transfer bandwidth of the device measured with PLL. Orange curve: experimental detection bandwidth of the device. Blue curve: transfer function of the PLL with a cut-off at  $\sim 1 \text{ MHz}$ . (b) Experimental estimation of the thermal diffusion time. When sweeping the modulation frequency of the QCL, the Amplitude response of the device (grey dots) can be well fitted by a delayed oscillator model (red line) with a delay time of  $\sim 1.2 \mu\text{s}$ .

The intrinsic limit of this type of detection scheme is set by a thermal diffusion time on the nano-beam. Assuming a 1-D thermal diffusion condition, the diffusion time  $\tau_D$  of the heat along the mechanical beam can be calculated from the Fick's law of diffusion [13]  $\tau_D = \frac{L^2}{D}$ , where  $L = \frac{l}{2}$  is the half-length of the mechanical beam and  $D = \frac{\lambda_T}{c\rho} \sim 6 \times 10^{-5} \text{ m}^2 \text{ s}^{-1}$  is the thermal diffusion coefficient with  $\lambda_T = 163 \text{ W m}^{-1} \text{ K}^{-1}$  the average thermal conductivity,  $c = 252 \text{ J kg}^{-1} \text{ K}^{-1}$  the average specific heat at constant pressure, and  $\rho = 11.3 \times 10^3 \text{ kg/m}^3$  the average density of the gold/GaAs beam. As a result, the thermal diffusion time  $\tau_D$  is calculated to be  $\sim 1.2 \mu\text{s}$ . In addition,  $\tau_D$  can also be estimated experimentally by sweeping the modulation frequency of the QCL and recording the amplitude response, as presented in Figure 3b (gray dots). This curve can be well fitted by a delayed oscillator model, which is the transfer function of a harmonic oscillator multiplied by that of a low-pass filter due to the retardation of the thermal diffusion, as introduced in ref [14]. Again, the thermal diffusion time extracted from the fitting (red curve) is  $\sim 1.2 \mu\text{s}$ , in excellent agreement with the analytical estimation. Therefore, we can conclude that the thermal diffusion time in our mechanical beam is on the order of  $1 \mu\text{s}$ , consistent with the response speed of  $\sim 1 \text{ MHz}$ .

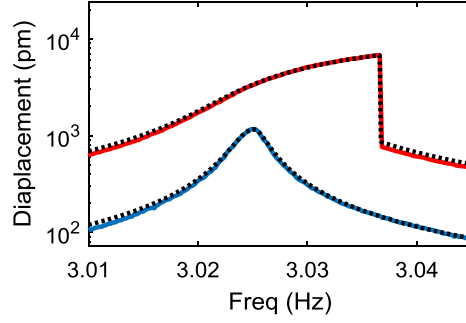


Figure 4: Linear (blue) and non-linear (red) amplitude responses of the device when sweeping 1V or 2.5V RF drive. The blue curve can be well fitted by a simple harmonic oscillator model while the red one needs to be fitted by a non-linear Duffin model.

In the PLL measurements, the dielectric force applied by the RF electrical field to the nano-beam can be estimated by considering the vibrating beam as an effective one-dimensional harmonic oscillator. While the driving force is distributed homogeneously along the beam section, it can be replaced by an effective force that is applied in the middle of the beam. In that condition, for a doubly-clamped rectangular beam, the effective mass of the 1D harmonic oscillator can be calculated as  $m_{eff} = 0.4\rho \cdot l \cdot w \cdot u = 6.7 \text{ pg}$ . The effective stiffness is then calculated as  $k_{eff} = m_{eff} \cdot (2\pi f)^2 = 2.2 \text{ N/m}$  with the resonance frequency  $f = 2.87 \text{ MHz}$  in our case. Therefore, the dielectric force applied onto the beam is expressed by  $F = \frac{k_{eff}}{Q} \Delta z \sim 3 \text{ pN}$ , in which the mechanical factor  $Q$  is 1000 and the displacement of the nano-beam  $\Delta z \sim 1160 \text{ pm}$ , as shown in Figure 4 (blue curve).

Increasing the driving force, one can set the system in the Duffin non-linear regime. In this regime, the system needs to be described by the Duffin equation  $\ddot{Y} + \frac{\omega_0}{Q} \dot{Y} + \omega_0^2 Y + \gamma Y^3 = F \cos(\omega_p t)$ , where  $\gamma \sim 1 \times 10^{29} \text{ m}^{-2} \text{ s}^{-2}$  is the Duffin constant and  $F$  is the driving force normalized to the effective mass of the oscillator. The value of the Duffin coefficient is exceptionally high in comparison to those reported in other systems with similar geometry [15]. As shown in Figure 4 (red curve), in the Duffin regime the system shows bi-state behaviour, jumping from a higher state down to the lower one at the critical frequency (here 3.037 MHz). This phenomenon can be exploited for applications such as logic gates, which is further studied in our ongoing work.

### 3 Conclusion

In this paper, we presented miniaturized optomechanical resonators that detect THz radiations at room temperature with a high responsivity of  $\sim 4 \text{ nm}/\mu\text{W}$ . Thanks to the miniaturized structure, our device has a short thermal diffusion time, on the order of  $\sim 1 \text{ }\mu\text{s}$ , allowing our device to work at a higher speed ( $\sim 1 \text{ MHz}$ ) than the other thermal detectors in previous reports. Therefore, our device can serve as a fast, sensitive THz detector to enable many applications such as THz imaging. It is also feasible to scale down our dog-bone design to implement optomechanical detectors working at other frequency ranges such as the mid-infrared [16]. In addition, our device can be driven into a strong nonlinear regime, serves as a great platform to study Duffing nonlinearity etc.

### References

- [1] I.F. Akyildiz, et al, Phys. Commun. 12, 16 (2014).
- [2] T. Nagatsuma, et al, Nat. Photonics 2016 106 10, 371 (2016).
- [3] M. Tonouchi, et al, Nat. Photonics 2007 12 1, 97 (2007).
- [4] R.A. Lewis, et al, J. Phys. D. Appl. Phys. 52, 433001 (2019).
- [5] F. Alves, et al, Opt. Express 21, 13256 (2013).
- [6] Y. Zhang, et al, J. Appl. Phys. 125, 151602 (2019).
- [7] C. Belacel, et al, Nat. Commun. 8, 2 (2017).
- [8] A. Calabrese, et al, Nanophotonics 8, 2269 (2019).

- [9] Q.P. Unterreithmeier, et al, Nature 458, 1001 (2009).
- [10] A.N. Cleland, et al, J. Appl. Phys. 92, 2758 (2002).
- [11] Zhang, X. C, ETAL, Nano Lett. 13 (4), 1528 (2013).
- [12] Calabrese, A. Optomechanical Terahertz Meta-Atoms, Université de Paris (2019).
- [13] Fick, A. V. On Liquid Diffusion . London, Edinburgh, Dublin Philos. Mag. J. Sci. (1855)
- [14] C. Metzger, et al, Phys. Rev. B, 78 (2008).
- [15] J.S. Huber, et al, Phys. Rev. X, 10 (2), 021066 (2020).
- [16] A. Benz, et al, Nat. Commun. 4, 2882 (2013).